Electronic Supplementary Material (ESI) for RSC Advances.

Supporting Information

The role of cation and anion dopant incorporated in a ZnO electron transporting layer for polymer bulk heterojunction solar cells

Soyeon Kim,[a] Jae Hoon Jeong,[a] Quoc Viet Hoang,[b] Joo Won Han,[c] Yong Hyun Kim,[c] Adi prasetio,[a,c], Muhammad Jahandar,[a] Shinuk Cho[d,*] and Dong Chan Lim[a,*]

[a]Surface Technology Division, Korea Institute of Materials Science (KIMS), 797 Changwondaero, Seongsan-gu, Changwon, Gyeongnam 51508, Republic of Korea.

[b]Vietnam-Korea Technological Innovation Center, Directorate for Standards, Metrology and Quality (STAMEQ), No.8 Hoang Quoc Viet, Cau Giay, Ha Noi, Vietnam

[c]Department of Display Engineering, Pukyong National University, Busan 48513, Republic of Korea.

[d]Department of Physics and EHSRC, University of Ulsan, Ulsan 44610, Republic of Korea.

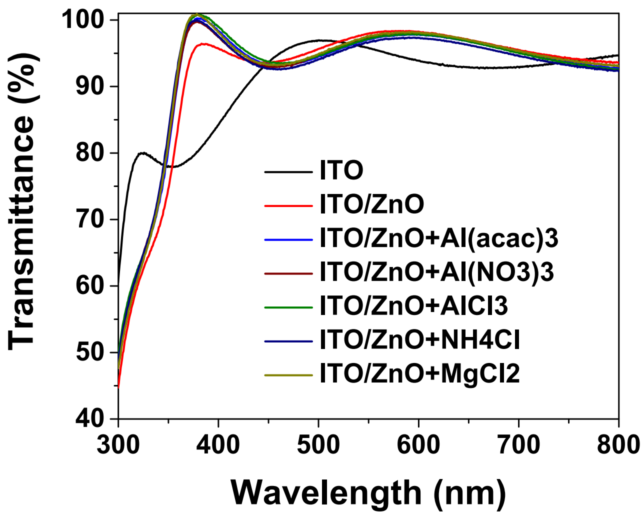

Figure S1. Optical transmittance spectra of different interlayers on a glass substrate and a lone glass substrate

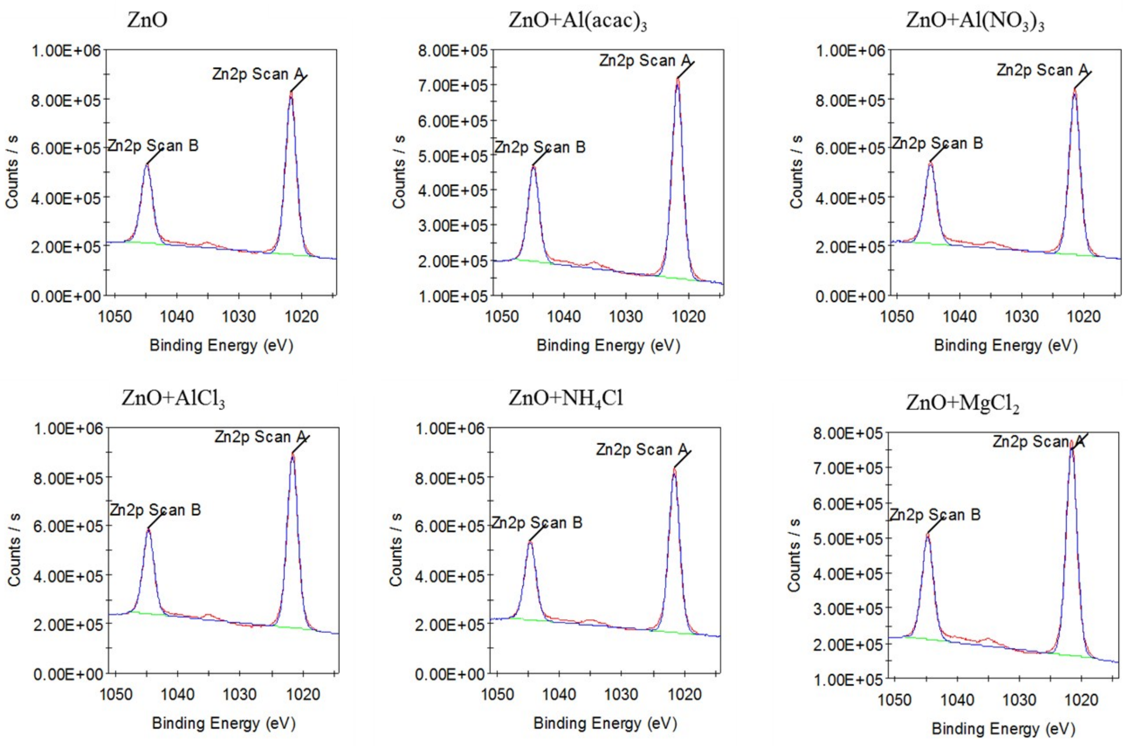

Figure S2. High-resolution XPS spectra of Zn 2p peaks of ZnO and doped ZnO layers on a silicon wafer

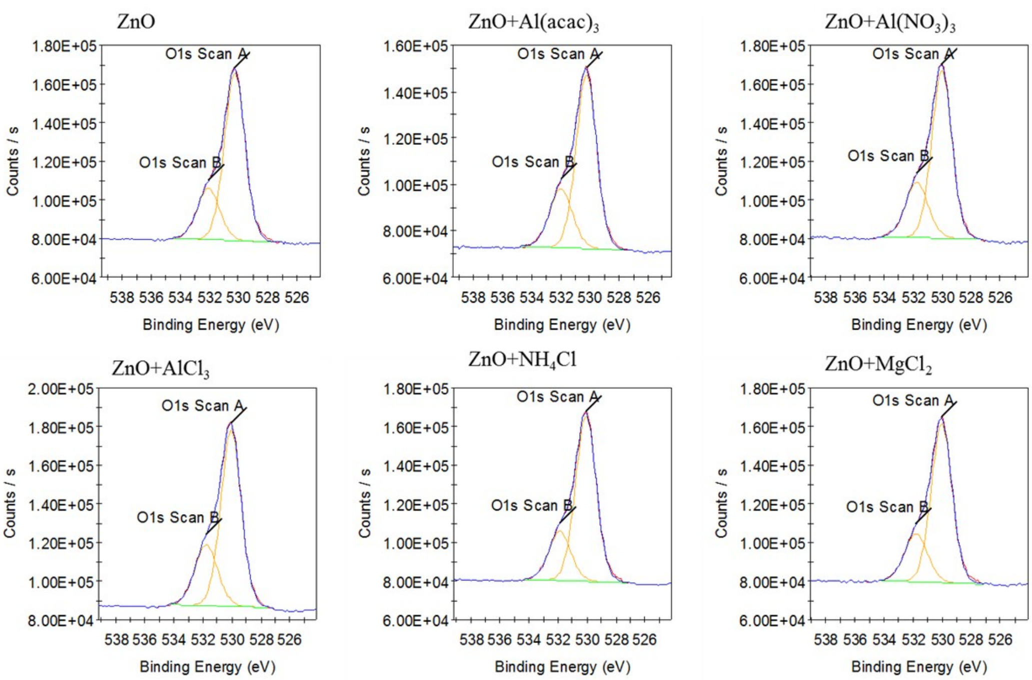

Figure S3. High-resolution XPS spectra of O 1s peaks of ZnO and doped ZnO layers on a silicon wafer

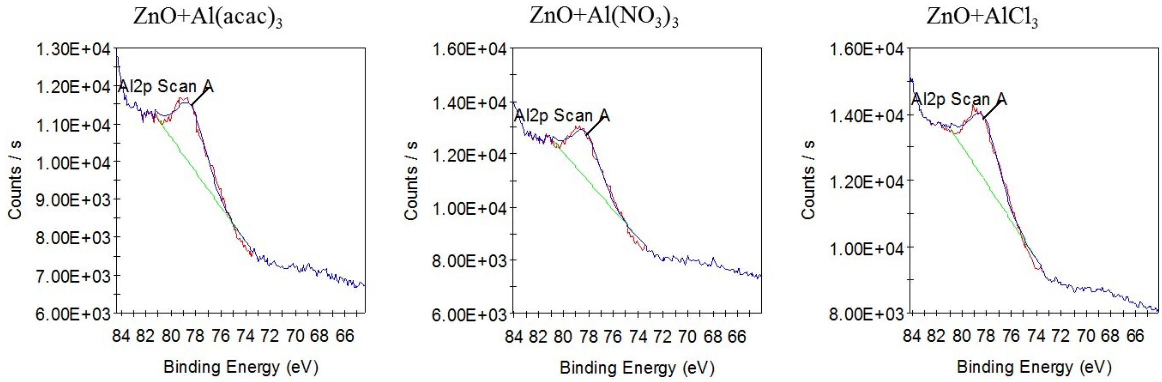

Figure S4. High-resolution XPS spectra of Al 2p peaks of doped ZnO thin films on a silicon wafer

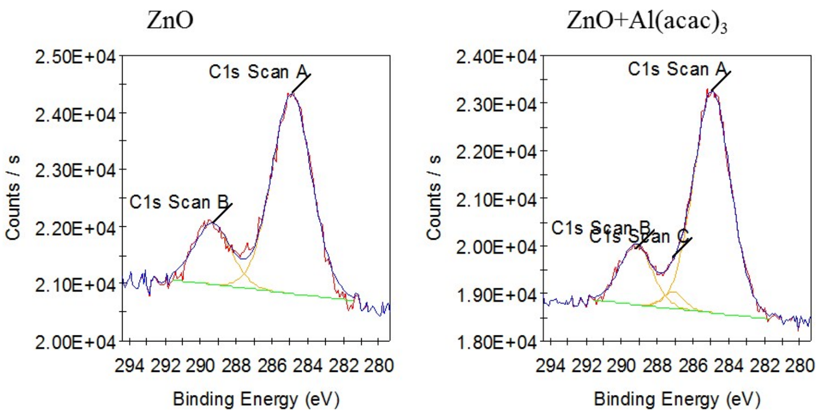

Figure S5. High-resolution XPS spectra of C 1s peaks of ZnO and Al(acac)$_3$-doped ZnO thin films on a silicon wafer

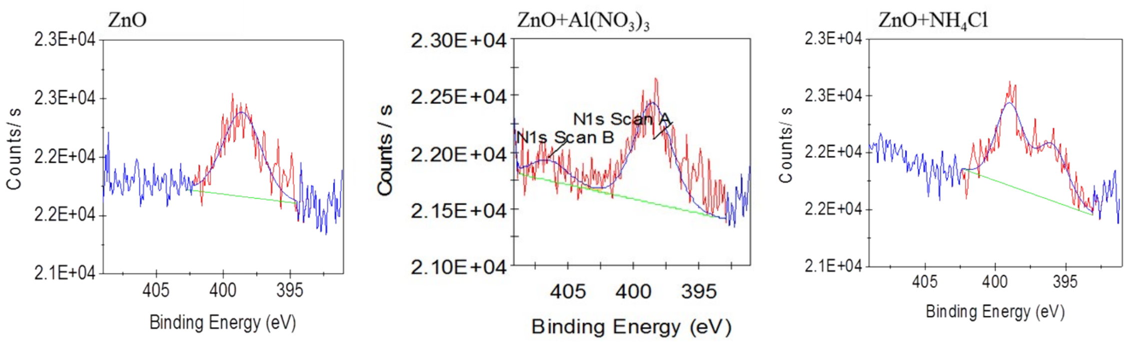

Figure S6. High-resolution XPS spectra of N 1s peaks of ZnO and doped ZnO thin films on a silicon wafer

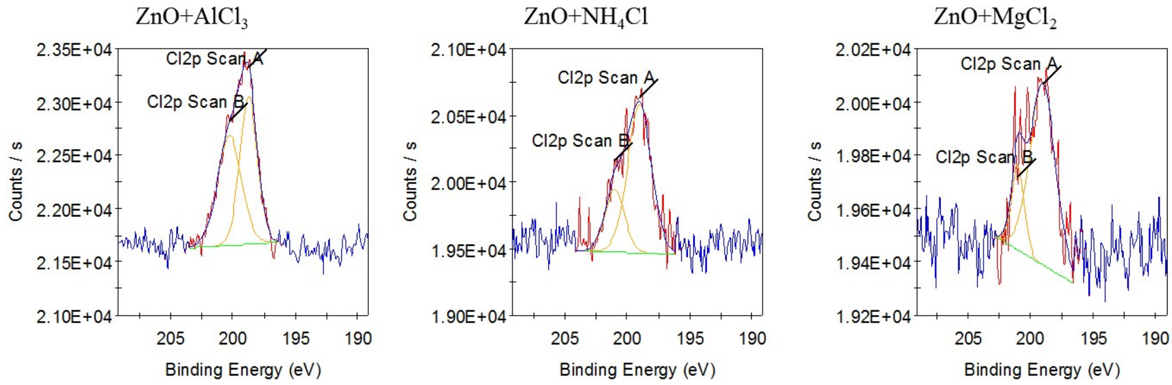

Figure S7. High-resolution XPS spectra of Cl 2p peaks of doped ZnO thin films on a silicon wafer

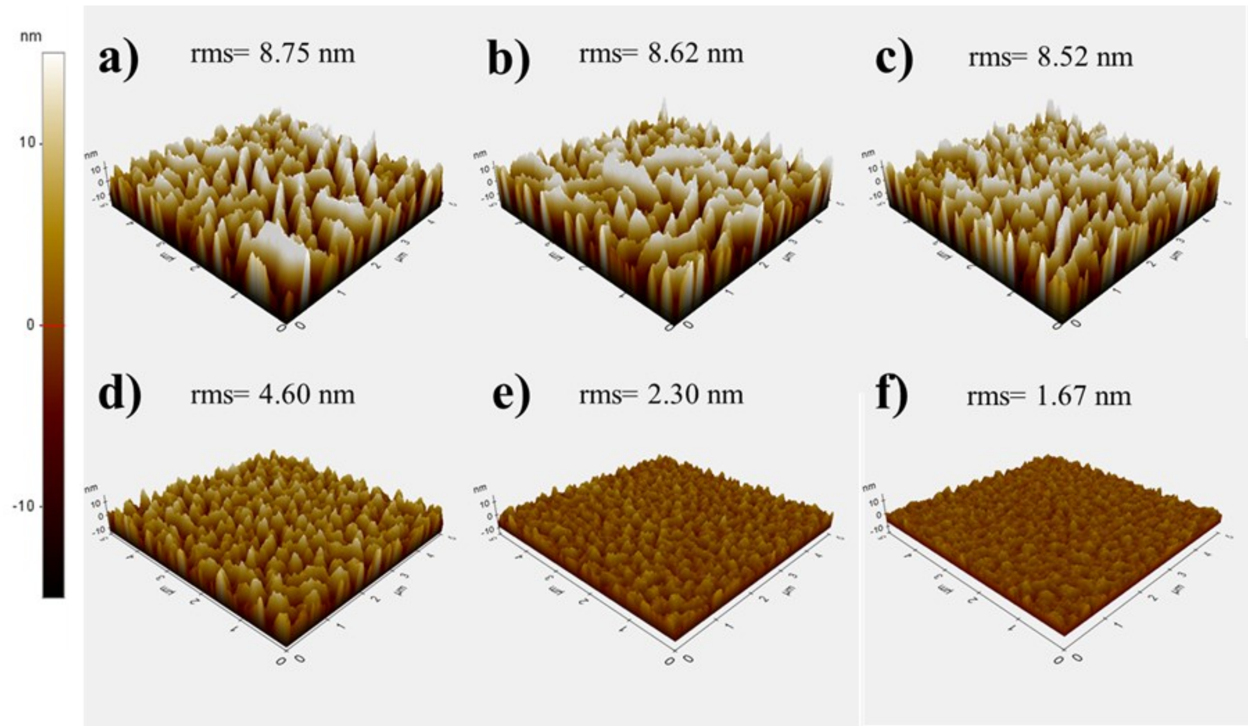

Figure S8: 3D AFM tapping-mode height images (5 µm x 5 µm) of a) ITO/ZnO; b)ITO/ZnO+ $Al(acac)_3$; c) ITO/ZnO+$Al(NO_3)_3$; d) ITO/ZnO+$AlCl_3$; e) ITO/ZnO+NH_4Cl; f) ITO/ZnO+$MgCl_2$

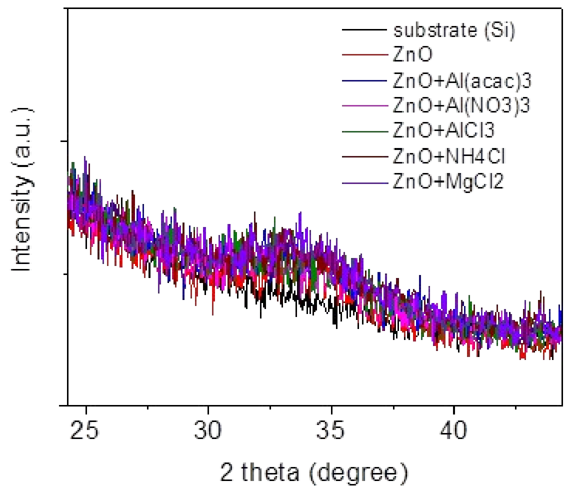

Figure S9. XRD of ZnO and doped ZnO thin films on a silicon wafer (annealing temperature: 180 ºC)

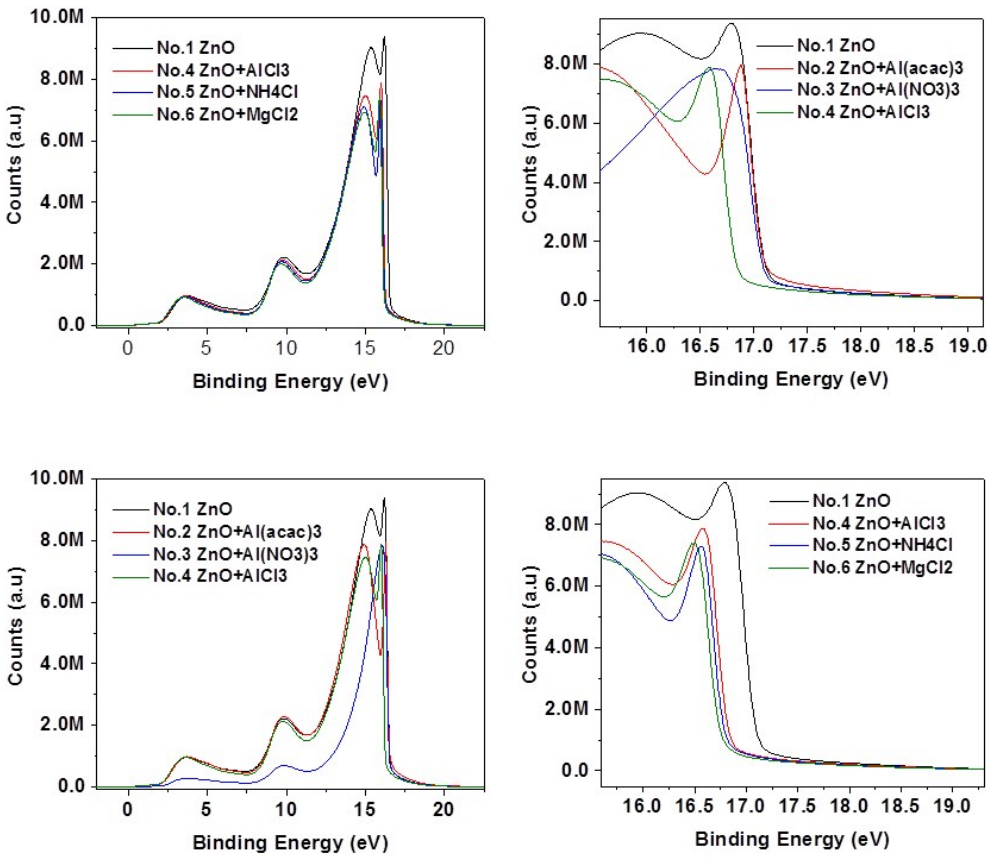

Figure S10: UPS spectra of interlayer thin films (Au substrate as a standard, WF =5.2 eV).

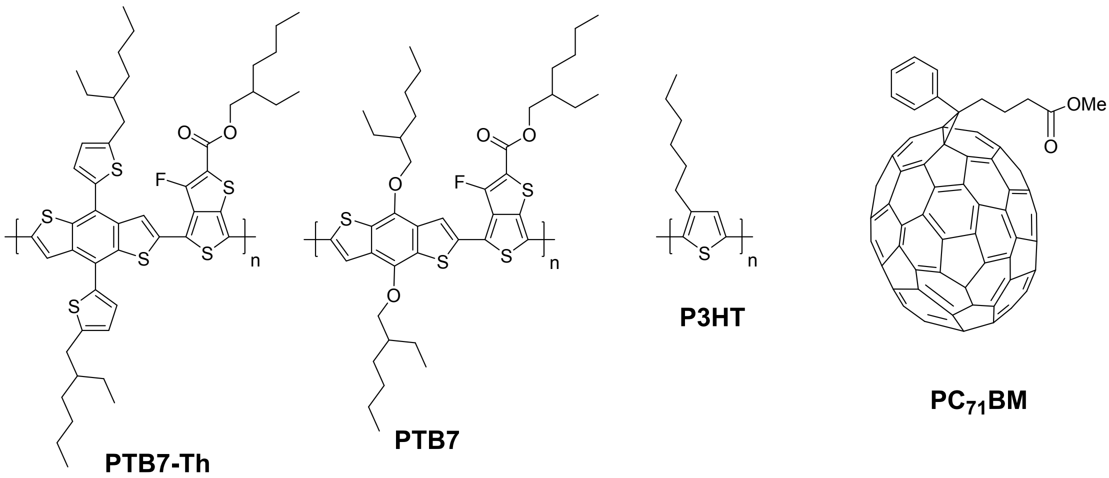

Figure S11. Polymer structures and $PC_{71}BM$

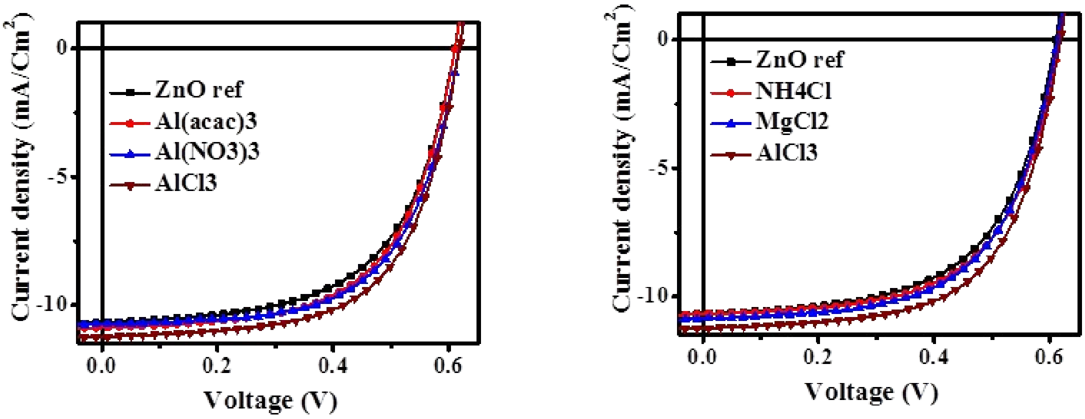

Figure S12. J-V curves of P3HT:$PC_{71}BM$ devices with different electron transporting layers.

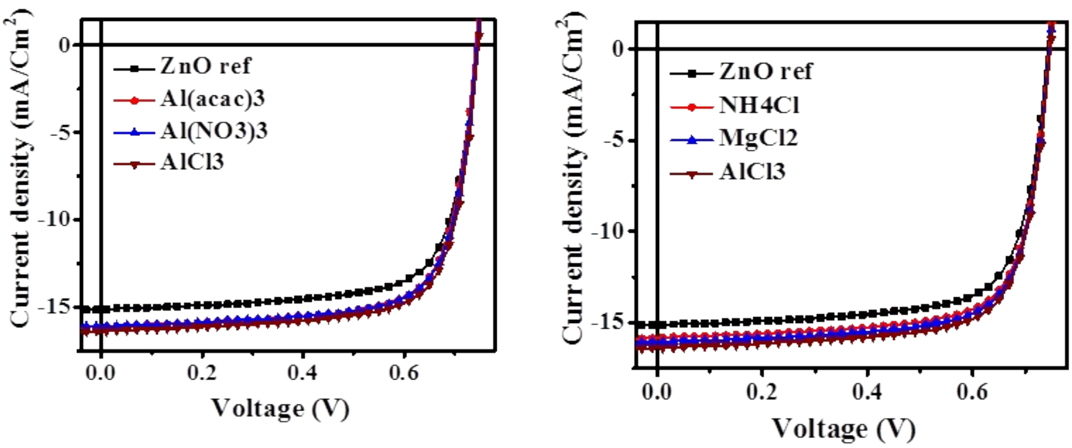

Figure S13. J-V curves of PTB7:$PC_{71}BM$ devices with different electron transporting layers.

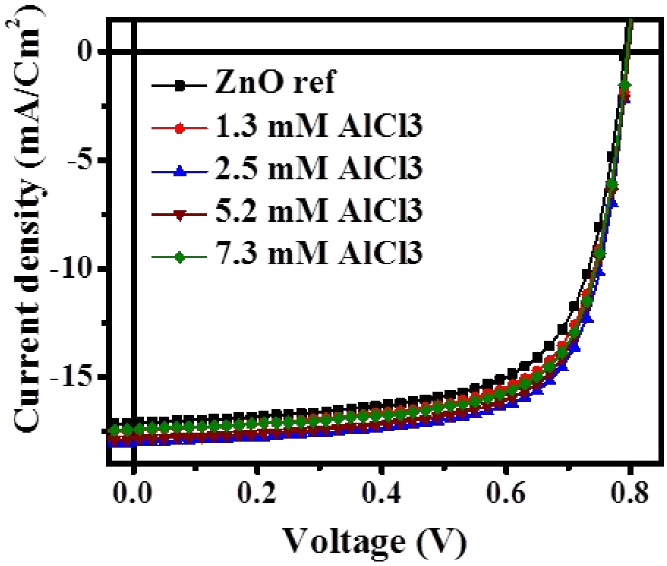

Figure S14. J-V curves of PTB7-Th:$PC_{71}BM$ devices with different $AlCl_3$ concentrations.

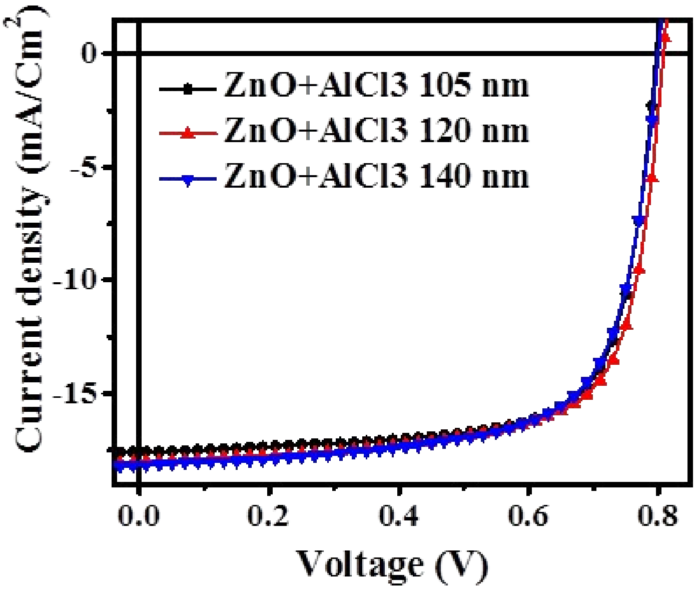

Figure S15. J-V curves of PTB7-Th:$PC_{71}BM$ devices with different active layer thicknesses. In these devices, the ZnO layer was doped with $AlCl_3$.

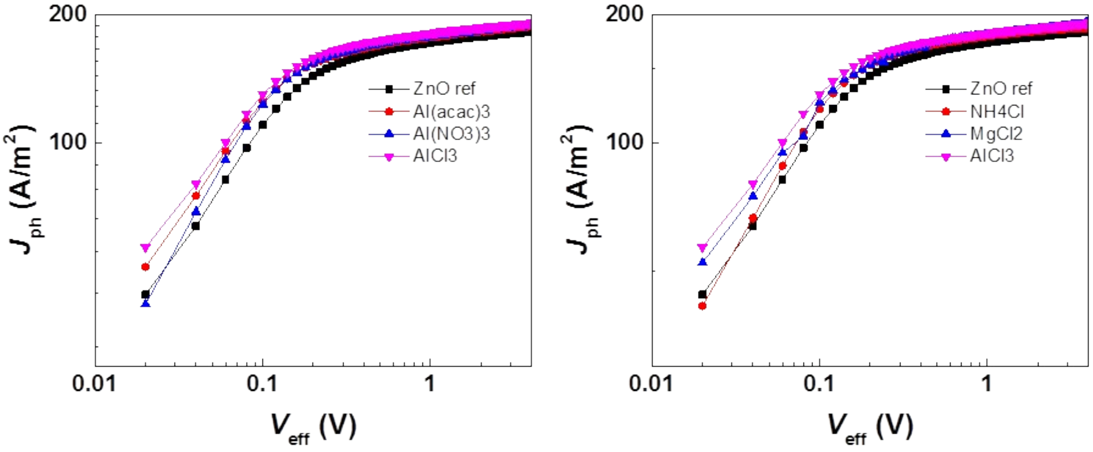

Figure S16. Photocurrents of PTB7-Th:PC$_{71}$BM devices with different electron transporting layers.

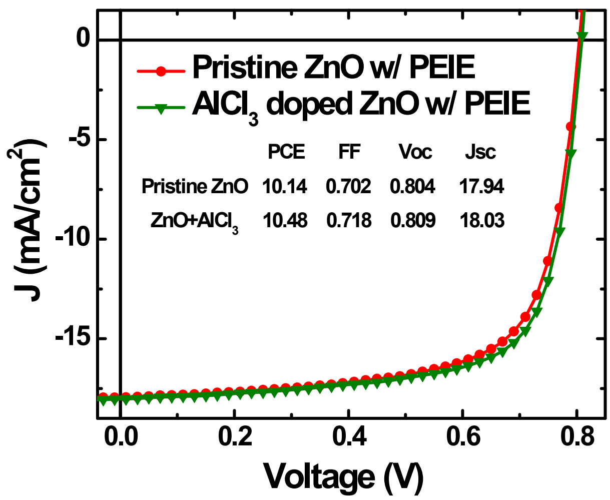

Figure S17. J-V curves of ZnO and AlCl$_3$-doped ZnO devices with PEIE as a surface modification layer.

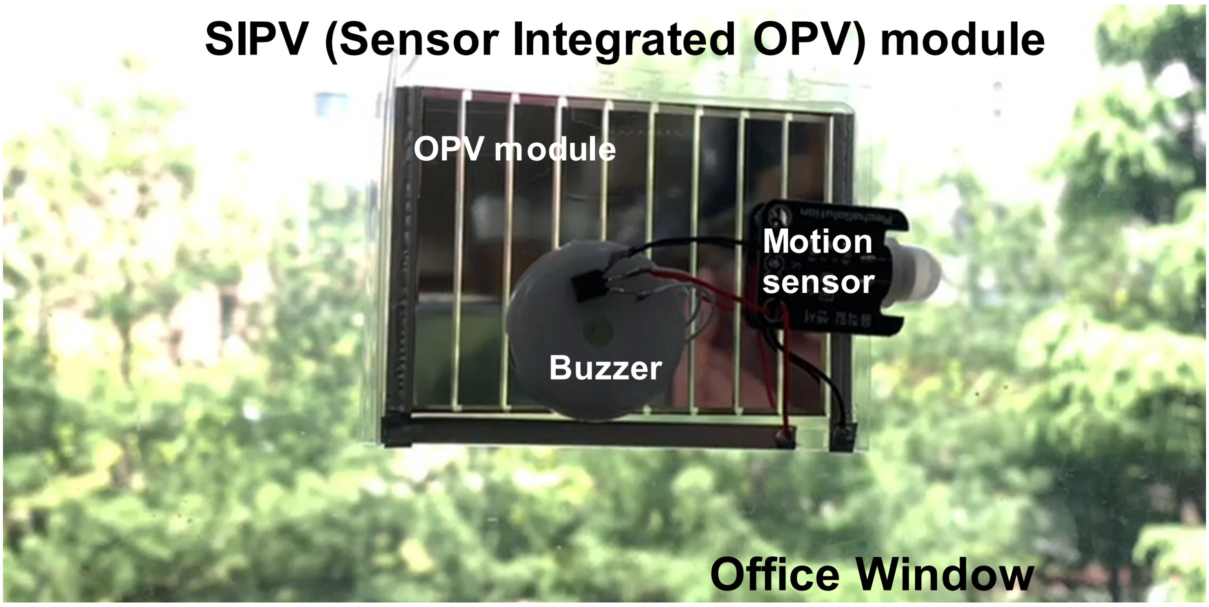

Figure S18. An organic solar module driven motion sensor device that includes an $AlCl_3$-doped ZnO ETL. An OPV module integrated with a motion sensor and buzzer is attached to the inside office window.

Table S1. Series resistances and shunt resistances are extracted from EIS fitting of PTB7-Th:$PC_{71}BM$ devices with different ETLs.

Device	Rs (Ohm)	Rsh (Ohm)
ZnO	10.4	28780
ZnO+$Al(acac)_3$	8.2	49990
ZnO+$Al(NO_3)_3$	6.2	29330
ZnO+$AlCl_3$	3.9	9080
ZnO+NH_4Cl	6.7	14510
ZnO+$MgCl_2$	6.5	10360

Table S2. Photovoltaic performances of P3HT:$PC_{71}BM$ devices with different electron transporting layers.

Device	PCE best (%)	F.F	Voc (V)	Jsc (mA/Cm^2)
Reference	3.84 (3.54) [a]	0.589	0.609	10.68
ZnO+$Al(acac)_3$	4.00 (3.71)	0.602	0.610	10.87
ZnO+$Al(NO_3)_3$	4.07 (3.85)	0.614	0.617	10.74
ZnO+$AlCl_3$	4.23 (4.02)	0.619	0.617	11.23
ZnO+NH_4Cl	3.97 (3.71)	0.604	0.615	10.67
ZnO+$MgCl_2$	4.02 (3.81)	0.604	0.612	10.86

[a] The average PCE from more than 8 devices.

Table S3. Photovoltaic performances of PTB7:$PC_{71}BM$ devices with different electron transporting layers.

Device	PCE best (%)	F.F	Voc (V)	Jsc (mA/Cm^2)
Reference	8.19 (7.78) [a]	0.729	0.742	15.13
ZnO+$Al(acac)_3$	8.74 (8.49)	0.731	0.741	16.11
ZnO+$Al(NO_3)_3$	8.79 (8.58)	0.733	0.744	16.08
ZnO+$AlCl_3$	9.01(8.85)	0.735	0.748	16.39
ZnO+NH_4Cl	8.68 (8.48)	0.735	0.745	15.82
ZnO+$MgCl_2$	8.82 (8.57)	0.735	0.746	16.07

[a] The average PCE from more than 8 devices.

Table S4. Photovoltaic performances of devices with different $AlCl_3$ concentrations in $AlCl_3$-doped ZnO.

Device	PCE (%)	F.F	Voc (V)	Jsc (mA/Cm^2)
Reference	9.16	0.68	0.79	17.10
0.5M ZnO+ 1.3 mM AlCl3	9.56	0.69	0.80	17.45
0.5M ZnO+ 2.5 mM AlCl3	10.16	0.71	0.80	18.00
0.5M ZnO+ 5.2 mM AlCl3	9.95	0.70	0.80	17.86
0.5M ZnO+ 7.3 mM AlCl3	9.72	0.70	0.79	17.42

Table S5. Photovoltaic performances of state of the art organic solar cells with various ETL having PTB7-Th:$PC_{70}BM$ active layer.

Device	PCE best (%)	F.F	Voc (V)	Jsc (mA/cm^2)	Ref.
ZnO	7.48	0.58	0.74	15.66	[1]
ZnO/PEI	9.67	0.68	0.79	16.52	
ZnO	8.81	0.63	0.79	17.23	[2]
ZnO/PEOz	9.57	0.68	0.80	18.10	
ZnO	9.50	0.67	0.78	17.50	[3]
ZnO/PFS-FTEG	10.60	0.72	0.80	18.30	
ZnO/PFS-FC	10.10	0.69	0.80	18.00	
TiO_2	9.49	0.69	0.79	17.25	[4]
PEI	9.62	0.67	0.77	18.57	
PFN-OX	9.44	0.66	0.78	18.11	
TiO_2/PEI	10.06	0.71	0.81	17.20	
PEI/TiO_2	10.30	0.71	0.81	17.64	
ZnO	9.16	0.67	0.79	17.10	This work
ZnO+$AlCl_3$	10.38	0.71	0.80	18.01	
ZnO/PEIE	10.14	0.70	0.80	17.94	
ZnO+$AlCl_3$/PEIE	10.48	0.71	0.80	18.03	

Reference:

[1] C. Wang, C. Li, R. C. I. Mackenzie, S. Wen, Y. Liu, P. Ma, G. Wang, W. Tian and S. Ruan, *J. Mater. Chem. A*, 2018, 6, 17662–17670.

[2] S. Nam, J. Seo, S. Woo, W. H. Kim, H. Kim, D. D. C. Bradley and Y. Kim, *Nat. Commun.*, 2015, 6, 8929.

[3] J. Subbiah, V. D. Mitchell, N. K. C. Hui, D. J. Jones and W. W. H. Wong, *Angew. Chem. Int. Ed.*, 2017, 56, 8431–8434.

[4] Y. Yan, F. Cai, L. Yang, W. Li, Y. Gong, J. Cai, S. Liu, R. S. Gurney, D. Liu and T. Wang, *ACS Appl. Mater. Interfaces*, 2017, 9, 32678–32687.